AGU ADVANCING EARTH AND SPACE SCIENCE

Geophysical Research Letters

RESEARCH LETTER
10.1029/2022GL102354

Impact of Extratropical Northeast Pacific SST on U.S. West Coast Precipitation

É. Beaudin[1], E. Di Lorenzo[1], A. J. Miller[2], H. Seo[3], and Y. Joh[4]

[1]Department of Earth, Environmental & Planetary Sciences, Brown University, Providence, RI, USA, [2]Scripps Institution of Oceanography, La Jolla, CA, USA, [3]Woods Hole Oceanographic Institution, Woods Hole, MA, USA, [4]Atmospheric and Oceanic Sciences, Princeton University, Princeton, NJ, USA

Key Points:

- Warming along the U.S. West Coast can induce wind-driven vapor fluxes changes leading to enhanced precipitation
- Extratropical sea surface temperature (SST) forcing can impact large-scale atmospheric circulation
- U.S. West Coast precipitation are impacted by extratropical Northeast Pacific SST

Supporting Information:

Supporting Information may be found in the online version of this article.

Correspondence to:

É. Beaudin,
elise_beaudin@brown.edu

Citation:

Beaudin, É., Di Lorenzo, E., Miller, A. J., Seo, H., & Joh, Y. (2023). Impact of extratropical Northeast Pacific SST on U.S. West Coast precipitation. *Geophysical Research Letters*, *50*, e2022GL102354. https://doi.org/10.1029/2022GL102354

Received 5 DEC 2022
Accepted 23 JAN 2023

Author Contributions:

Conceptualization: É. Beaudin, E. Di Lorenzo, A. J. Miller, H. Seo
Data curation: É. Beaudin
Formal analysis: É. Beaudin
Funding acquisition: E. Di Lorenzo
Investigation: É. Beaudin
Methodology: É. Beaudin, E. Di Lorenzo, H. Seo
Project Administration: E. Di Lorenzo
Resources: É. Beaudin
Software: É. Beaudin
Supervision: E. Di Lorenzo, A. J. Miller, H. Seo
Validation: É. Beaudin
Visualization: É. Beaudin, Y. Joh
Writing – original draft: É. Beaudin

Abstract The rainfall over the U.S. West Coast is known to be highly influenced by large-scale atmospheric circulation and tropical climate teleconnections. However, the role of North Pacific oceanic variability is less understood. Using high-resolution regional atmospheric model simulations forced by sustained positive and negative phases of the extratropical Pacific Decadal Oscillation sea surface temperature anomalies (SSTa), we diagnose the precipitation changes over the U.S. West Coast during 2010–2020. We find that precipitation anomalies are up to 60% stronger (weaker) for the warm (cold) cases, especially over Northern and Central California during wintertime, and Baja California in the summertime. In both seasons, precipitation is predominantly modulated through changes in the water vapor flux, which are directed toward the coast in wintertime and away from the coast during summertime. These flux anomalies are primarily driven by large-scale changes in the wind associated with the atmospheric adjustment to the strong ocean SSTa.

Plain Language Summary This study examines how ocean temperature in the Northeast Pacific affects rainfall in the U.S. West Coast using computer model simulations over the period 2010–2020. Rainfall generally increases when coastal waters are warmer and vice versa. This is especially true in Northern and Central California during wintertime and in Baja California during summertime. The amount of rain is mainly affected by changes in the water vapor that moves toward the coast in the winter and away from the coast in the summer. These changes in water vapor are caused by changes in the wind, which are linked to changes in the surface ocean temperature.

1. Introduction

Precipitation over the U.S. West Coast is influenced by coupled processes between the sea surface temperature (SST) and atmospheric circulation (Hu et al., 2021) with a large fraction of its variability controlled by natural mid-latitude atmospheric processes (Williams et al., 2015; B. Dong & Dai, 2015). While previous studies have mostly focused on the role of tropical SST on regional climate in the U.S. (e.g., Alexander et al. (2002)), the role of extratropical SST forcing on precipitation over land remains less understood, although as been somewhat explored (Liu et al., 2021). Predicting precipitation over the U.S. West Coast has always been a challenge, and it is of utmost importance for water management with California being the largest agricultural producer in the United States.

Previous studies have shown that SST can influence precipitation through atmospheric teleconnections, by increasing the transport of warm and wet flow from over the ocean to land, thus enhancing precipitation rates (Barron et al., 2012; L. Dong et al., 2018; Hu et al., 2021; Livezey & Smith, 1999; Zhang et al., 2010). Over the Northeast Pacific sector, the most influential mode of interannual variability is El Nino-Southern Oscillation (ENSO). The warm phase of ENSO increases chances of extreme precipitation during winter over southwestern U.S. (Zhang et al., 2010). Even though tropical SST forcing does play a major role in modulating precipitation, there is growing evidence that extratropical SST variability may play an additionally important role and lead to enhanced predictability (Cheng et al., 2021; Dai, 2013; Wei et al., 2021; Zhang et al., 2010).

It is still an open question of how strongly extratropical SST impacts precipitation over the U.S. West Coast (e.g., Persson et al. (2005)). With the global climate undergoing rapid changes and most regions getting warmer, anomalous SST events such as marine heatwaves (MHWs) are projected to increase in intensity, duration, and frequency (Frölicher et al., 2018; Viglione, 2021). During 2010–2020 the Northeast Pacific experiences a very strong warm anomalous state with three unprecedented extreme events such as the multi-year 2013–2015 Northeast Pacific

Writing – review & editing: É. Beaudin, E. Di Lorenzo, A. J. Miller, H. Seo, Y. Joh

MHW (Bond et al., 2015; Di Lorenzo & Mantua, 2016), the strong 2015 El Nino (Jacox et al., 2016), and the 2019 Alaskan heatwave (Amaya, 2019). These extreme events have been linked to changes in landfall precipitation over the U.S. West Coast through atmospheric teleconnections and are connected to the dynamics of the large-scale climate modes such as the Pacific Decadal Oscillation (PDO) and the North Pacific Gyre Oscillation (NPGO) (see review by Di Lorenzo et al. (2023)). For example, during the multi-year 2013–2015 MHW, one of the worst droughts was observed over the U.S. West Coast, especially over California (Griffin & Anchukaitis, 2014; Seager et al., 2015). It is still unclear whether the extratropical ocean conditions contributed to the drought or if they were merely a symptom of the drought.

The wet season over the U.S. West Coast typically starts in October and ends in April (L. Dong et al., 2019; Swain et al., 2015). Rainfall during this time of the year mostly comes from extratropical storms in the North Pacific via the jet stream. The storm track position is influenced by SST changes along the western boundary of the North Pacific Ocean (Hoskins & Valdes, 1990; Kuwano-Yoshida & Minobe, 2017), as well as global scale atmospheric circulation. During summer, as the heat builds up on land, a high-pressure system forms over the U.S. southwest, bringing onshore winds from the Gulf of California with a strong moisture influx contributing to summer monsoonal precipitation (Kim et al., 2005), called the North American Monsoon (NAM). While monsoonal precipitation is strongest over Mexico, rain also falls over California (Mitchell et al., 2002).

In this study, we explore the potential influence of persistent, strong extratropical SST changes on precipitation over the U.S. West Coast. We selected the extratropical expression of the PDO pattern as a proxy for the sea surface temperature anomalies (SSTa) expression of MHWs over the Northeast Pacific based on the studies of Di Lorenzo and Mantua (2016) and Xu et al. (2021), which show how the dynamical evolution of MHWs in this region typically evolves into PDO-like pattern. While previous studies have explored the connection of the PDO dynamics onto US hydroclimate, here the PDO pattern is only used as a proxy for warmer SSTa that are used to explore the role of extratropical SSTa on hydroclimate variability that is independent of the tropical forcing. Moreover, there have been suggestions that the variance of PDO may be increasing under global warming (Di Lorenzo & Mantua, 2016; Joh & Di Lorenzo, 2017). The fundamental role of the atmosphere in driving the PDO has previously been clearly identified (Newman et al., 2016; Schneider & Cornuelle, 2005). Few studies, however, have addressed the potential feedback role of the corresponding persistent extratropical ocean anomalies on changes in precipitation over land. We investigate the role of the Northeast Pacific SST on precipitation over the U.S. West Coast using regional atmospheric model simulations designed to isolate the potential impact of large-scale, persistent, strong MHW, here represented by the PDO pattern as a prototype for assessing sensitivities. We aim to identify the spatial patterns of changes in precipitation over land associated with the warm and cold phases of the PDO, and the mechanisms forcing those changes.

2. Data, Model, and Experiments

2.1. Data Sets

Observations of precipitation are monthly mean computed from the Climate Prediction Center (CPC) Unified Gauge-Based Analysis of Daily Precipitation data set [0.5 × 0.5 horizontal grid] of the National Oceanic and Atmospheric Administration (NOAA) CPC product (M. Chen et al., 2008). This data set goes from 1941 to 2018. Wind data for model validation comes from the Coupled Ocean Atmosphere Mesoscale Prediction System Wind at 10 m, 4 km resolution (Doyle et al., 2009). The PDO was reconstructed using the PDO index from NOAA (Mantua & Hare, 2002), as well as the sea-surface temperature (SST) data from the Hadley Center Sea Ice and Sea Surface Temperature data set (Rayner, 2003). We used the ERA5 reanalysis product (Hersbach et al., 2020) with a 30 km horizontal grid resolution for the boundary conditions for the model experiments. The variables used at 6 hr time steps were zonal and meridional winds, temperature, relative, specific humidity, and geopotential at 30 levels from 1,000 to 50 hPa, as well as surface winds, soil, water and 2 m air temperature, and pressure.

2.2. Model Description

We carried out a set of continuous 10-years simulations using the Weather Research and Forecasting (WRF, Skamarock et al. (2021)) to assess the impact of the Northeast Pacific SST on U.S. precipitation. WRF is a state-of-the-art mesoscale numerical weather prediction model designed for both atmospheric research and weather forecasting (https://www.mmm.ucar.edu/models/wrf). It can resolve small scale and mesoscale dynamics,

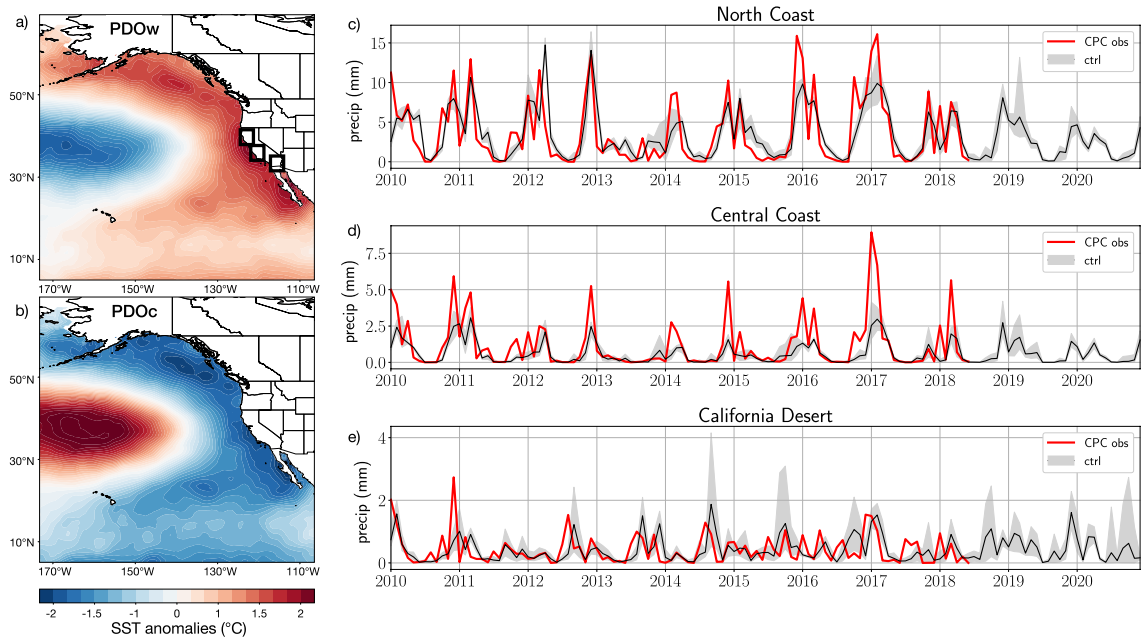

Figure 1. PDO-shaped warm (a) and cold (b) sea surface anomalies patterns (a), (b) used for the experiment. Precipitation during 2010–2020 (c, d, e) of the model ensemble output (black line) and observations (red line) for three key California regions. The gray shading represents the ensemble spread. Each region is indicated by a box in (a).

with several choices of physical parameterizations including microphysics, cumulus parameterization, planetary boundary layer (PBL), land-surface models (LSM), and longwave and shortwave radiation. For this study, the Thompson parameterization (Thompson et al., 2008) was chosen for microphysics, the rapid radiative transfer model scheme (Mlawer et al., 1997) for longwave radiation, the Dudhia scheme (Dudhia, 1989) for shortwave radiation, Noah LSM scheme (F. Chen & Dudhia, 2001) for land-surface, the Kain-Fritsch scheme (Kain, 2004) for the cumulus parameterization, and the Yonsei University (YSU) scheme (Hong et al., 2006) for the PBL parameterization.

The atmospheric domain comprises the whole Northeast Pacific Ocean, from −180° to −110° longitude and 5° to 67° latitude (Figure 1a), including Hawaii, the southern part of Alaska, and about half of the North American continent. The horizontal spatial resolution is 1/4°, which corresponds to 25 km around the equator. We used 44 vertical levels from the surface to 50 hPa. The basic state initial conditions and surface and lateral boundary conditions were interpolated from the ERA5 global reanalysis data set with a 6-hourly time interval. All simulations were carried out for the period 2010–2020, with daily outputs from which monthly means were computed.

2.3. Experimental Setup

2.3.1. Control Run

An 8-member ensemble was generated using WRF for the basic state (observed SST) conditions. Each member has slightly different initial conditions to assess potential nonlinearities in the internal variability of the regional system. The first timestep of every January months of the control run was used for the initial SST map. For example, 1st January 2011, was the initial SST map of the second ensemble member, and the year 2012 for the third ensemble member, and so on. The resulting ensemble spread was very small, indicating that the boundary conditions largely controlled the atmospheric flows in the domain for fixed SST. Since the boundary controls were so strong, the ensemble spread of the control was assumed to represent the ensemble spread of the SST anomaly runs and was used to assess the statistical significance of differences between cases.

2.3.2. Validation

The model output was validated by comparing several variables, including temperature, zonal and meridional winds, and precipitation, with observations and reanalysis products at sea level pressure, 500 and 200 hPa (see

Figures S1–S4 in Supporting Information S1). In general, our model data was in good agreement with the observations. Moreover, the model spread is relatively small among the ensemble members, which tells us that the boundary conditions dominate the internal variability in our domain. The results were deemed sufficiently realistic to proceed with the perturbation SST runs.

2.3.3. Sensitivity Tests

We conducted two separate SST anomaly experiments, one by superimposing a warm phase PDO spatial anomalies onto the prescribed time dependent SSTa surface boundary conditions and another one using the cold phase (Figures 1a and 1b) for the same time period as the control run. The PDO anomaly pattern was reconstructed by creating a composite SST map of when the PDO index amplitude exceeded ±1 standard deviation. The maximum amplitudes of our warm/cool patterns were then scaled to ±2C to simulate the occurrence of extremes, which typically of this order in the Northeast Pacific. Note that this technique does not produce perfectly symmetric PDO warm (PDOw) and PDO cold (PDOc) patterns due to the retention of random SST variations during the construction of the composites. The SST patterns of the PDO are shown in Figures 1a and 1b and indicate strong similarity with the PDO EOF pattern (Mantua & Hare, 2002). We refer to those two experiments as PDOw and PDOc.

2.3.4. Analysis

Using the precipitation model output, we compared monthly averaged data with observation to first evaluate the accuracy of the data set. We computed the monthly climatology to find the months where the warm and cold experiments would exceed the ensemble spread. The months of March and September showed the strongest responses in precipitation anomaly. The anomalies for the PDOw and PDOc experiments are calculated with respect to the ensemble mean. To determine the mechanisms by which precipitation over land was influenced by the SST, we looked at changes in the relation between anomalies of precipitation, winds, moisture content, and integrated vapor transport (IVT) where IVT indicates the direction and amplitude of the water vapor flux over a region:

$$\mathbf{IVT} = \frac{1}{g}\int_{surface}^{300mb} Q\mathbf{U}dp \tag{1}$$

For the analysis, we separated the IVT anomalies into a velocity (U) perturbation term and a water vapor (Q) perturbation term:

$$(QU)' = Q'\bar{U} + \bar{Q}U' + Q'U' + \overline{Q'U'} \tag{2}$$

The terms on the right side of the equation are the water vapor anomalies advected by the mean flow, the wind anomalies acting on the mean water vapor distribution, the eddy fluxes associated with wind anomalies acting on water vapor anomalies, and the mean eddy fluxes. Differences in variables between cases were deemed to be statistically significant if they exceeded 2 standard deviations of the ensemble spread.

2.3.5. Statistical Testing

We applied a significance test for correlations and regressions in this paper, based on the Probability Density Function (PDF) method. The PDF was constructed using the Monte Carlo method, using 1,000 pairs of random red noise time series with a decorrelation length of 3 months, which corresponds to that of the data.

3. Results

3.1. Simulated and Observed Precipitation Over North America

The 2010–2020 model precipitation is compared with observations in Figures 1c, 1d, and 1e, averaged over three key climate regions of California: the North Coast, the Central Coast and the California Desert. The modeled precipitation timeseries compare favorably with the observations with significant correlation above the 95% level (see Figure 1). It is also important to note that precipitation is not a state variable, but rather a prognostic variable that is dependent on the choice of physics parameterizations.

Inspection of the timeseries reveals that the model is able to reproduce the seasonal cycle, with precipitation peaking during wintertime and nearing zero during summertime. However, the model produces less rainfall

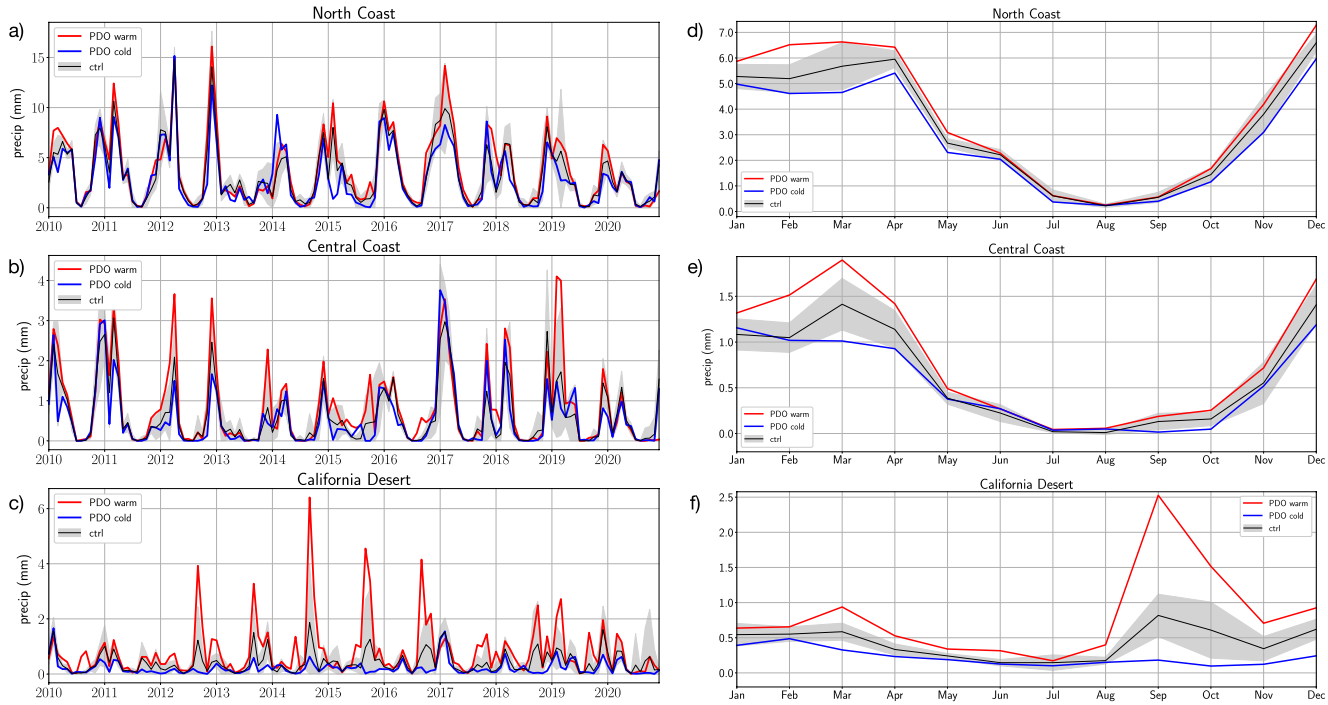

Figure 2. Time series of precipitation for the control (black line and shading), the warm (red) and cold (blue) experiments, in the North Coast, Central Coast and California Desert (locations indicated in boxes on Figure 1). The left panels (a, b, c) show the full time series during 2010–2020, and the right panels (d, e, f) show the corresponding seasonal cycle.

than observed as evident when comparing the ensemble spread (gray lines) with the observational data (red line) in Figure 1. The years 2013–2015 show reduced precipitation in both observations and the model, consistent with the multi-year 2013–2015 North Pacific MHW during which atmospheric conditions tremendously reduced precipitation over California. Large differences in model versus observed precipitation are sometimes found during the wet seasons, particularly in 2017. Given that the model captures the precipitation seasonal cycle over key regions of the U.S. West Coast, we assume that the model has sufficient verisimilitude to be used for further analysis on how extratropical SST warming impacts coastal precipitation.

3.2. Sensitivity of Precipitation to SST Warming and Cooling

The sensitivity of coastal precipitation to the persistent, strong, warming patterns for PDOw and PDOc are shown in Figure 2, for three different regions in California over the period 2010–2020 (left panel). The seasonal cycle (right panel) was computed by averaging the 11 years for each month. We find that the PDOw experiment is wetter and the PDOc experiment is drier over the course of the runs. The wetter and drier conditions are significant when the red (PDOw) and blue (PDOc) curves are outside the gray envelope of the ensemble spread. Precipitation differences during the wintertime are greatest during the month of March for all three regions. The late summer precipitation is greatly enhanced in the California Desert region for the PDOw anomalies, hinting that warming along the coast impacts the monsoon precipitation. Summer precipitation is barely impacted in the North and Central Coasts. The mechanisms behind those changes are investigated in the next section. For the analysis, we focus on the months of March and September to study the contrast between winter and summer precipitation, as these months were the most significantly impacted.

3.3. Mechanisms of Precipitation Changes

To understand the mechanism behind the changes in precipitation, we first examine anomalies of precipitation, winds, geopotential height, and IVT. Given that the month of March was found to be the most impacted in terms of precipitation anomalies in the wintertime, we examine its precipitation spatial anomalies pattern over the Northeast Pacific (Figures 3a and 3d). We find that the anomalies in March resemble the SST anomaly patterns

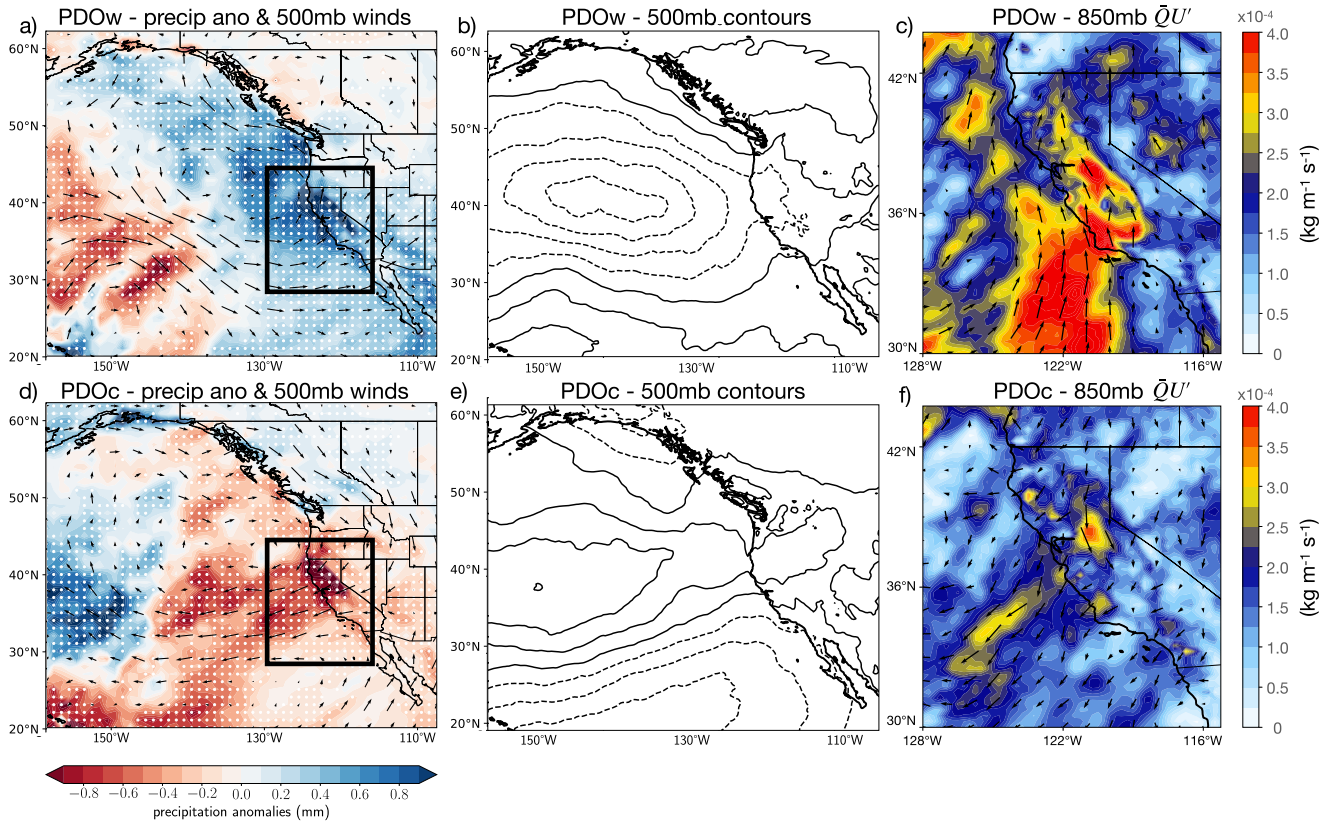

Figure 3. March anomalies for the warm (a, b, c) and cold (d, e, f) experiments. Precipitation anomalies (shading) and 500 mb winds anomalies (vectors) (a), (d), 500 mb geopotential height anomalies (b), (e), and QU' term at 925 mb (c), (f) zoomed over the region shown in the box.

of the PDOw and PDOc used in the sensitivity run (Figures 1a and 1b). Specifically, drier conditions are found over regions of colder SST anomalies, and wetter conditions are found over regions of warmer SST anomalies. For the PDOw experiment, the strongest winter signal of increased precipitation is centered off the U.S. West Coast and over northern California. This area underlies a 2,000 km-scale cyclonic flow in the 500 mb winds, also present when looking at the 500 mb geopotential height (Figure 3b). This is consistent with the warm SST in that area producing rising air and cyclonic circulation. We chose to show the winds at 500 mb since they are equivalent barotropic to at least 500 mb. For PDOc, the strongest signal of decreased precipitation extends from over California far offshore into the subtropical gyre. This area underlies the southern flanks of a 2,000 km-scale anticyclonic flow in 500 mb winds, which is also represented by the 500 mb geopotential height (Figure 3e). This flow is consistent with the cool SST in that area producing sinking air and anticyclonic circulation. March composite precipitation anomalies range from −1.1 to 1.9 mm for the PDOw experiment, and from −1.8 to 1.6 mm for the PDOc experiment. The strongest anomalies over land are found over northern California in both cases where changes in onshore and offshore wind directions associated with the atmospheric circulation changes appear to be critical in determining the sign of the precipitation response. Southern California is only slightly impacted. The local 500 mb wind fields indicate anomalous onshore flow for PDOw and anomalous offshore flow for PDOc.

To further diagnose the relative importance of the processes contributing to precipitation, we separated the mean water vapor flux into three terms QU′, Q′U, and Q′U′ (see Figures S7–S10 in Supporting Information S1), and found that QU′ (Figures 3c and 3f) dominates the other terms, which have magnitudes of about 2–3 times smaller. The local surface IVT anomalies over California (Figures 3c and 3f) indicate that there are onshore moisture flux anomalies for PDOw and offshore moisture flux anomalies for PDOc. The IVT anomalies impacting California are dominated by changes in anomalous wind, and only weakly influenced by the anomalous water vapor. Thus, the mechanism controlling the enhanced rainfall for the PDOw case is enhanced water vapor flux brought by the anomalous wind driven by the large-scale cyclonic flow over the Northeast Pacific (and vice versa for PDOc),

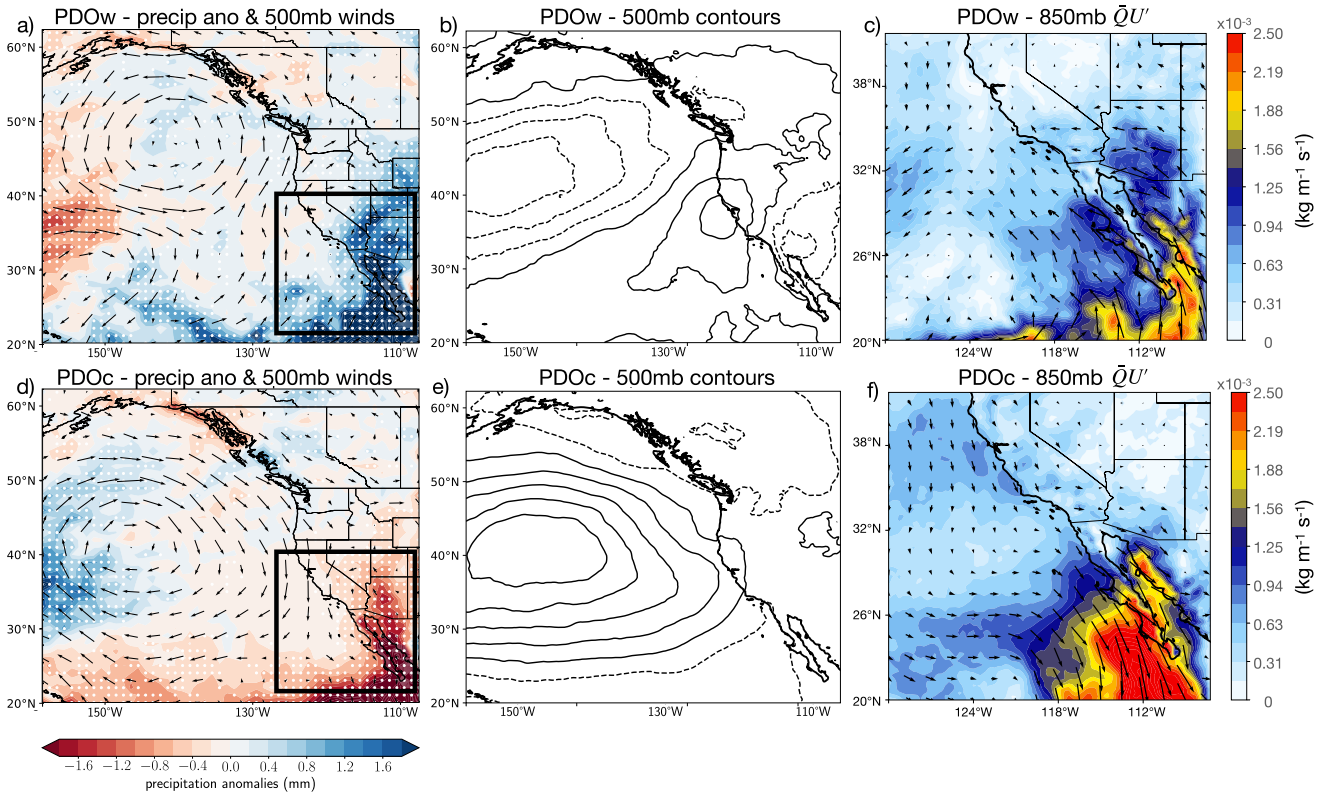

Figure 4. September anomalies for the warm (a, b, c) and cold (d, e, f) experiments. Precipitation anomalies (shading) and 500 mb winds anomalies (vectors) (a), (d), 500 mb geopotential height anomalies (b), (e), and QU′ term at 925 mb (c), (f) zoomed over the region shown in the box.

and a small portion of the altered moisture transport is attributed to a change in the anomalous water vapor concentration.

During summertime (Figure 4), precipitation anomalies are surprisingly found to be much stronger than in winter, ranging from −1.6 to 12.9 mm for the PDOw, and from −7.8 to 2.5 mm for the PDOc. The important precipitation anomalies over land are found over southern California and Baja California in Mexico, which is where the NAM region is located. A closer look at the $\bar{Q}U'$ term over the U.S. Southwest demonstrates the enhanced moisture flux is mainly influenced by the anomalous wind which is onshore for PDOw and offshore for PDOc. The PDOc anomalous wind is clearly a result of the large-scale anticyclonic pattern brought by colder SST over the Northeast Pacific, which drives water vapor flux away from Southern California (Figure 4f). This explains the strong decrease in rainfall over southern California during summertime.

4. Summary and Discussion

This study assesses the sensitivity of the U.S. West Coast precipitation to changes in North Pacific SST. We used a modeling approach in which two different scenarios were compared to an 8-members ensemble of a regional atmospheric model. For the two sensitivity simulations, we superimposed a PDO-like pattern of SST to the pre-existing temperatures, one positive and one negative. We ran the model for the period 2010–2020 and looked at a climatology of precipitation anomalies. These model results demonstrate that there is a potentially significant contribution to precipitation over land from strong, persistent, large-scale midlatitude SST anomalies of the North Pacific.

Both experiments showed that the state of California was the most significantly impacted by the warming patterns; the north in winter and the south in summer. These differences in location can be explained through the different position of the large-scale pressure system anomalies created by the warming/cooling patterns.

During wintertime, studies found that precipitation along the coast is sensitive to changes in SST and latent heat fluxes (Bartusek et al., 2021; X. Chen & Leung, 2020; Persson et al., 2005). However, our finding suggests that

this is not the main mechanism by which precipitation over California is impacted by large-scale North Pacific SSTa. We partitioned the thermodynamic and dynamic contributions of the water vapor flux anomalies and found that wind anomalies are the dominant driver for the observed changes in precipitation. The warm experiment demonstrated that by increasing SST along the coast and decreasing SST in the center of the Northeast Pacific, this creates a large-scale cyclonic flow barotropic to at least 500 mb. Those wind anomalies thus enhance water vapor flux over northern California, causing an increase in precipitation. In contrast, the cold experiment demonstrates how colder SSTs along the U.S. West Coast and warmer in the center of the Northeast Pacific decreases the amount of moisture transported over land, thus decreasing precipitation. This change in precipitation is due to wind anomalies from a large-scale anticyclonic flow over the North Pacific caused by the perturbation in SSTs.

Summertime precipitation anomalies over land are strongest over the southwest U.S., and much larger than the winter anomalies. Composite analysis reveals that in both the warm and cold experiment, once again, the anomalous wind is the dominant factor for the large increase in precipitation over land. This dynamical adjustment also happens for the cold experiment in summertime, in the opposite direction. IVT anomalies are large and directed away from the shore, thus greatly reducing precipitation over southern California.

The Clausius-Clapeyron relation, which relates the increase in water vapor with increasing air temperature, would predict a thermodynamic adjustment. It does play a role, but both wintertime and summertime precipitation anomalies seem to be primarily modulated through a dynamical adjustment brought by a large-scale alteration in SSTs in the Northeast Pacific which changes the large-scale atmospheric circulation. In both seasons, warming along the coast caused more landfall precipitation. Pascale et al. (2017) investigated how projected changes in atmospheric warming due to increased levels of CO_2 would impact the North American Monsoonal system. They found that Monsoonal precipitation is amplified by SST warming patterns, associated with decreased atmospheric stability. This is consistent with our findings, as we found that a dynamical adjustment happens when warming the coast, which effectively increases precipitation over the Monsoon-impacted region, notably over the California Desert. Moreover, previous work with coarser coupled climate modeling explore the relation between SSTa in the California Current upwelling system and the hydroclimate over North America during the Pliocene, and found that warmer regional ocean SSTa lead to wetter conditions over land (Fu et al., 2022).

Finally, it is important to recognize that warming or cooling the whole Northeast Pacific with a PDO-like pattern, and thus adding infinite heat capacity for this whole period, is unrealistic. However, this study does not aim at linking the specifics of the PDO to precipitation anomalies, but rather to give an insight on how extratropical SST anomalies can potentially have an impact on precipitation over the U.S. West Coast. Given that midlatitude air-sea coupling could be a driver for changes in precipitation over California, this motivates additional research on possible impacts on coastal precipitation associated with extreme warming events in the Northeast Pacific, which often have oceanic patterns that resemble the expression of the climate modes such as PDO and the North Pacific Gyre Oscillation (NPGO).

Data Availability Statement

The modeled atmospheric data to reproduce the figures from this study is available at https://doi.org/10.5281/zenodo.7401465.

Acknowledgments
We thank the NSF for supporting this study under the Grants GR-5216036, OCE-2022846, OCE-2306046, and OCE-2022868.

References

Alexander, M. A., Bladé, I., Newman, M., Lanzante, J. R., Lau, N.-C., & Scott, J. D. (2002). The atmospheric bridge: The influence of ENSO teleconnections on air–sea interaction over the global oceans. *Journal of Climate*, *15*(16), 2205–2231. https://doi.org/10.1175/1520-0442(2002)015⟨2205:TABTIO⟩2.0.CO;2

Amaya, D. J. (2019). The Pacific meridional mode and ENSO: A review. *Current Climate Change Reports*, 5(4), 296–307. https://doi.org/10.1007/s40641-019-00142-x

Barron, J. A., Metcalfe, S. E., & Addison, J. A. (2012). Response of the North American monsoon to regional changes in ocean surface temperature: Holocene SSTS and NAM expression. *Paleoceanography*, *27*(3), PA3206. https://doi.org/10.1029/2011PA002235

Bartusek, S. T., Seo, H., Ummenhofer, C. C., & Steffen, J. (2021). The role of nearshore air-sea interactions for landfalling atmospheric rivers on the. U.S. West Coast, *48*(6), e2020GL091388. https://doi.org/10.1029/2020GL091388

Bond, N. A., Cronin, M. F., Freeland, H., & Mantua, N. (2015). Causes and impacts of the 2014 warm anomaly in the NE Pacific: 2014 warm anomaly in the NE Pacific. *Geophysical Research Letters*, *42*(9), 3414–3420. https://doi.org/10.1002/2015GL063306

Chen, F., & Dudhia, J. (2001). Coupling an advanced land surface–hydrology model with the Penn state–NCAR MM5 modeling system. Part I: Model implementation and sensitivity. *Monthly Weather Review*, *129*(4), 569–585. https://doi.org/10.1175/1520-0493(2001)129⟨0569:CAALSH⟩2.0.CO;2

Chen, M., Shi, W., Xie, P., Silva, V. B. S., Kousky, V. E., Wayne Higgins, R., & Janowiak, J. E. (2008). Assessing objective techniques for gauge-based analyses of global daily precipitation. *Journal of Geophysical Research*, *113*(D4), D04110. https://doi.org/10.1029/2007JD009132

Chen, X., & Leung, L. R. (2020). Response of landfalling atmospheric rivers on the U.S. West Coast to local sea surface temperature perturbations. *Geophysical Research Letters*, *47*(18), e2020GL089254. https://doi.org/10.1029/2020GL089254

Cheng, R., Novak, L., & Schneider, T. (2021). Predicting the interannual variability of California's total annual precipitation. *Geophysical Research Letters*, *48*(7), e2020GL091465. https://doi.org/10.1029/2020GL091465

Dai, A. (2013). The influence of the inter-decadal Pacific oscillation on US precipitation during 1923–2010. *Climate Dynamics*, *41*(3), 633–646. https://doi.org/10.1007/s00382-012-1446-5

Di Lorenzo, E., Xu, T., Zhao, Y., Newman, M., Capotondi, A., Stevenson, S., et al. (2023). Modes and mechanisms of Pacific decadal-scale variability. *Annual Review of Marine Science*, *15*(1), 249–275. https://doi.org/10.1146/annurev-marine-040422-084555

Di Lorenzo, E., & Mantua, N. (2016). Multi-year persistence of the 2014/15 north Pacific marine heatwave. *Nature Climate Change*, *6*(11), 1042–1047. https://doi.org/10.1038/nclimate3082

Dong, B., & Dai, A. (2015). The influence of the interdecadal Pacific oscillation on temperature and precipitation over the globe. *Climate Dynamics*, *45*(9), 2667–2681. https://doi.org/10.1007/s00382-015-2500-x

Dong, L., Leung, L. R., Lu, J., & Song, F. (2019). Mechanisms for an amplified precipitation seasonal cycle in the U.S. West Coast under global warming. *Journal of Climate*, *32*(15), 4681–4698. https://doi.org/10.1175/JCLI-D-19-0093.1

Dong, L., Leung, L. R., Song, F., & Lu, J. (2018). Roles of SST versus internal atmospheric variability in winter extreme precipitation variability along the U.S. West Coast. *Journal of Climate*, *31*(19), 8039–8058. https://doi.org/10.1175/JCLI-D-18-0062.1

Doyle, J. D., Jiang, Q., Chao, Y., & Farrara, J. (2009). High-resolution real-time modeling of the marine atmospheric boundary layer in support of the AOSN-II field campaign. *Deep Sea Research Part II: Topical Studies in Oceanography*, *56*(3), 87–99. https://doi.org/10.1016/j.dsr2.2008.08.009

Dudhia, J. (1989). Numerical study of convection observed during the winter monsoon experiment using a mesoscale two-dimensional model. *Journal of the Atmospheric Sciences*, *46*(20), 3077–3107. https://doi.org/10.1175/1520-0469(1989)046<3077:nsocod>2.0.co;2

Frölicher, T. L., Fischer, E. M., & Gruber, N. (2018). Marine heatwaves under global warming. *Nature*, *560*(7718), 360–364. https://doi.org/10.1038/s41586-018-0383-9

Fu, M., Cane, M. A., Molnar, P., & Tziperman, E. (2022). Warmer Pliocene upwelling site SST leads to wetter subtropical coastal areas: A positive feedback on SST. *Paleoceanography and Paleoclimatology*, *37*(2), e2021PA004357. https://doi.org/10.1029/2021PA004357

Griffin, D., & Anchukaitis, K. J. (2014). How unusual is the 2012-2014 California drought? *Geophysical Research Letters*, *41*(24), 9017–9023. https://doi.org/10.1002/2014GL062433

Hersbach, H., Bell, B., Berrisford, P., Hirahara, S., Horányi, A., Muñoz-Sabater, J., et al. (2020). The ERA5 global reanalysis. *Quarterly Journal of the Royal Meteorological Society*, *146*(730), 1999–2049. https://doi.org/10.1002/qj.3803

Hong, S.-Y., Noh, Y., & Dudhia, J. (2006). A new vertical diffusion package with an explicit treatment of entrainment processes. *Monthly Weather Review*, *134*(9), 2318–2341. https://doi.org/10.1175/MWR3199.1

Hoskins, B. J., & Valdes, P. J. (1990). On the existence of storm-tracks. *Journal of the Atmospheric Sciences*, *47*(15), 1854–1864. https://doi.org/10.1175/1520-0469(1990)047<1854:oteost>2.0.co;2

Hu, F., Zhang, L., Liu, Q., & Chyi, D. (2021). Environmental factors controlling the precipitation in California. *Atmosphere*, *12*(8), 997. https://doi.org/10.3390/atmos12080997

Jacox, M. G., Hazen, E. L., Zaba, K. D., Rudnick, D. L., Edwards, C. A., Moore, A. M., & Bograd, S. J. (2016). Impacts of the 2015-2016 El Niño on the California current system: Early assessment and comparison to past events: 2015-2016 El Niño impact in the CCS. *Geophysical Research Letters*, *43*(13), 7072–7080. https://doi.org/10.1002/2016GL069716

Joh, Y., & Di Lorenzo, E. (2017). Increasing coupling between NPGO and PDO leads to prolonged marine heatwaves in the northeast Pacific. *Geophysical Research Letters*, *44*(22), 11663–11671. https://doi.org/10.1002/2017GL075930

Kain, J. S. (2004). The Kain–Fritsch convective parameterization: An update. *Journal of Applied Meteorology*, *43*(1), 170–181. https://doi.org/10.1175/1520-0450(2004)043⟨0170:TKCPAU⟩2.0.CO;2

Kim, J., Kim, J., & Farrara, J. D. (2005). The effects of the gulf of California SSTs on warm-season rainfall in the southwestern United States and northwestern Mexico. *18*, 24.

Kuwano-Yoshida, A., & Minobe, S. (2017). Storm-track response to SST fronts in the northwestern Pacific region in an AGCM. *Journal of Climate*, *30*(3), 1081–1102. https://doi.org/10.1175/JCLI-D-16-0331.1

Liu, X., Ma, X., Chang, P., Jia, Y., Fu, D., Xu, G., et al. (2021). Ocean fronts and eddies force atmospheric rivers and heavy precipitation in western North America. *Nature Communications*, *12*(1), 1268. https://doi.org/10.1038/s41467-021-21504-w

Livezey, R. E., & Smith, T. M. (1999). Covariability of aspects of North American climate with global sea surface temperatures on interannual to interdecadal timescales. *Journal of Climate*, *12*(1), 14–302. https://doi.org/10.1175/1520-0442-12.1.289

Mantua, N. J., & Hare, S. R. (2002). The Pacific decadal oscillation. *Journal of Oceanography*, *58*(1), 35–44. https://doi.org/10.1023/a:1015820616384

Mitchell, D. L., Ivanova, D., Rabin, R., Brown, T. J., & Redmond, K. (2002). Gulf of California sea surface temperatures and the North American monsoon: Mechanistic implications from observations. *Journal of Climate*, *15*(17), 2261–2281. https://doi.org/10.1175/1520-0442(2002)015⟨2261:GOCSST⟩2.0.CO;2

Mlawer, E. J., Taubman, S. J., Brown, P. D., Iacono, M. J., & Clough, S. A. (1997). Radiative transfer for inhomogeneous atmospheres: RRTM, a validated correlated-k model for the longwave. *Journal of Geophysical Research*, *102*(D14), 16663–16682. https://doi.org/10.1029/97JD00237

Newman, M., Alexander, M. A., Ault, T. R., Cobb, K. M., Deser, C., Di Lorenzo, E., et al. (2016). The Pacific decadal oscillation, revisited. *Journal of Climate*, *29*(12), 4399–4427. https://doi.org/10.1175/JCLI-D-15-0508.1

Pascale, S., Boos, W. R., Bordoni, S., Delworth, T. L., Kapnick, S. B., Murakami, H., et al. (2017). Weakening of the North American monsoon with global warming. *Nature Climate Change*, *7*(11), 806–812. https://doi.org/10.1038/nclimate3412

Persson, P. O. G., Neiman, P. J., Walter, B., Bao, J.-W., & Ralph, F. M. (2005). Contributions from California coastal-zone surface fluxes to heavy coastal precipitation: A CALJET case study during the strong. El Niño of 1998. *Monthly Weather Review*, *133*(5), 1175–1198. https://doi.org/10.1175/MWR2910.1

Rayner, N. A. (2003). Global analyses of sea surface temperature, sea ice, and night marine air temperature since the late nineteenth century. *Journal of Geophysical Research*, *108*(D14), 4407. https://doi.org/10.1029/2002JD002670

Schneider, N., & Cornuelle, B. D. (2005). The forcing of the Pacific decadal oscillation. *Journal of Climate*, *18*(21), 4355–4373. https://doi.org/10.1175/JCLI3527.1

Seager, R., Hoerling, M., Schubert, S., Wang, H., Lyon, B., Kumar, A., et al. (2015). Causes of the 2011–14 California drought. *Journal of Climate*, *28*(18), 6997–7024. https://doi.org/10.1175/JCLI-D-14-00860.1

Skamarock, W. C., Klemp, J. B., Dudhia, J., Gill, D. O., Liu, Z., Berner, J., et al. (2021). A description of the advanced research WRF model version 4 (p. 165).

Swain, D. L., Lebassi-Habtezion, B., & Diffenbaugh, N. S. (2015). Evaluation of nonhydrostatic simulations of northeast Pacific atmospheric rivers and comparison to in situ observations. *Monthly Weather Review*, *143*(9), 3556–3569. https://doi.org/10.1175/MWR-D-15-0079.1

Thompson, G., Field, P. R., Rasmussen, R. M., & Hall, W. D. (2008). Explicit forecasts of winter precipitation using an improved bulk microphysics scheme. Part II: Implementation of a new snow parameterization. *Monthly Weather Review*, *136*(12), 5095–5115. https://doi.org/10.1175/2008MWR2387.1

Viglione, G. (2021). Sudden fevers are gripping parts of the ocean with increasing frequency. Scientists are scrambling to forecast them and prevent harm to marine life, *593*(7857), 26–28. https://doi.org/10.1038/d41586-021-01142-4

Wei, W., Yan, Z., & Li, Z. (2021). Influence of Pacific decadal oscillation on global precipitation extremes. *Environmental Research Letters*, *16*(4), 044031. https://doi.org/10.1088/1748-9326/abed7c

Williams, A. P., Seager, R., Abatzoglou, J. T., Cook, B. I., Smerdon, J. E., & Cook, E. R. (2015). Contribution of anthropogenic warming to California drought during 2012–2014. *Geophysical Research Letters*, *42*(16), 6819–6828. https://doi.org/10.1002/2015GL064924

Xu, T., Newman, M., Capotondi, A., & Di Lorenzo, E. (2021). The continuum of northeast Pacific marine heatwaves and their relationship to the tropical Pacific. *Geophysical Research Letters*, *48*(2), e2020GL090661. https://doi.org/10.1029/2020GL090661

Zhang, X., Wang, J., Zwiers, F. W., & Groisman, P. Y. (2010). The influence of large-scale climate variability on winter maximum daily precipitation over North America. *Journal of Climate*, *23*(11), 2902–2915. https://doi.org/10.1175/2010JCLI3249.1